PAPER

Check for updates

Photomechanical response under physiological conditions of azobenzene-containing 4D-printed liquid crystal elastomer actuators†

Lorena Ceamanos, [ID] [a] Dirk J. Mulder, [b] Zehra Kahveci, [a] María López-Valdeolivas, [a] Albert P. H. J. Schenning [ID] [bc] and Carlos Sánchez-Somolinos [ID] ★[ad]

Soft and mechanically responsive actuators hold the promise to revolutionize the design and manufacturing of devices in the areas of microfluidics, soft robotics and biomedical engineering. In many of these applications, the actuators need to operate in a wet environment that can strongly affect their performance. In this paper, we report on the photomechanical response in a biological buffer of azobenzene-containing liquid crystal elastomer (LCE)-based actuators, prepared by four-dimensional (4D) printing. Although the photothermal contribution to the photoresponse is largely cancelled by the heat withdrawing capacity of the employed buffer, a significant photoinduced reversible contraction, in the range of 7% of its initial length, has been achieved under load, taking just a few seconds to reach half of the maximum contraction. Effective photomechanical work performance under physiological conditions has, therefore, been demonstrated in the 4D-printed actuators. Advantageously, the photomechanical response is not sensitive to salts present in the buffer differently to hydrogels with responses highly dependent on the fluid composition. Our work highlights the capabilities of photomechanical actuators, created using 4D printing, when operating under physiological conditions, thus showing their potential for application in the microfluidics and biomedical fields.

1. Introduction

Soft actuators based on stimuli-responsive materials are gaining growing interest in the fields of microfluidics and healthcare technologies.[1–6] Their integration in these sectors has the potential to bring innovative design and production solutions for new advanced devices that need to be increasingly complex and reliable, yet faster, smaller and cost-effective. In many occasions, these actuators need to operate in contact with fluids. As an example, in microfluidic devices, actuators typically interact with liquids to promote their mixing or transport them through small channels and chambers and thus perform specific tasks for applications such as DNA amplification, diagnostics or genomics, among others.[1–3] Also, in minimally invasive interventions, catheters incorporating actuators need to operate within the bloodstream to remove blood clots, insert implants or locally administrate a drug.[4] As an evolution of these tethered catheter-based technologies, future small-scale untethered micro- and milli-robots will need to integrate actuators to get controlled access to highly delicate and difficult-to-reach regions inside the human body and perform diagnostic and therapeutic tasks.[5,6] In all these cases, contact of the actuators with fluids could have a large impact on the actuator's performance.

In this context, hydrogels, undergoing large volume changes due to swelling and deswelling in response to an external stimulus, such as heat, light or chemical, have been explored to implement actuators for these wet environments. However, hydrogels typically have limited mechanical strength and a response, in the order of minutes, that is highly dependent on the chemical components incorporated in the working fluid, these being strong limitations for the use of these materials in many applications.[7,8] Liquid crystal networks (LCNs), on the other hand, allow the preparation of dynamic structures capable of adapting their shape in response to different stimuli, performing considerable mechanical work when actuated and displaying significantly faster response times than those reached with

a Instituto de Nanociencia y Materiales de Aragón (INMA), CSIC-Universidad de Zaragoza, Departamento de Física de la Materia Condensada, Zaragoza, 50009, Spain. E-mail: carlos.s@csic.es

b Laboratory of Stimuli-responsive Functional Materials and Devices (SFD), Department of Chemical Engineering and Chemistry, Eindhoven University of Technology, P.O. Box 513, 5600 MB Eindhoven, The Netherlands

c Institute for Complex Molecular Systems, Eindhoven University of Technology, P.O. Box 513, 5600 MB Eindhoven, The Netherlands

d Centro de Investigación Biomédica en Red de Bioingeniería, Biomateriales y Nanomedicina, Instituto de Salud Carlos III, 50018 Zaragoza, Spain

† Electronic supplementary information (ESI) available. See DOI: https://doi.org/10.1039/d2tb02757g

hydrogels.[9] Besides, LCNs may be actuated in both water and air environments.[10] These materials exhibit anisotropic deformation as a result of a change in the molecular order of the constituent mesogens, induced by an external stimulus such as heat, light, pH or an electrical field.[11,12] Among these stimuli, light is especially attractive for the above-mentioned applications, as it allows remote actuation of these systems with excellent spatial and temporal control of excitation.[1,13–16]

Light-responsive LCNs can be synthesized by incorporating azobenzene units into a liquid crystal (LC) polymer network.[13,16–19] When exposed to light, macroscopic shape changes have been previously reported for azobenzene containing LCNs operated in air as a result of two main contributions: the photochemical effect and the photothermal effect. On the one hand, the photochemical effect has its origin in the fact that irradiation of azobenzene molecules with light at the absorption peak of the *trans* isomer (365 nm) leads to isomerization from the elongated *trans* to the bulky *cis* isomer, causing a decrease in the molecular order of the network.[10,15,20,21] The photothermal contribution, on the other hand, arises from the photon energy absorbed by the chromophore that is transformed into thermal energy, contributing to the order disruption of the LCN.[10,22] For both mechanisms, it needs to be considered that light intensity throughout the sample thickness is not uniform, as dictated by the Beer's law, due to the absorption of light at the illuminated side of the sample.[11,18,23] As a consequence, when one side of an LCN element with uniaxial oriented molecules is irradiated with ultraviolet (UV) light, this gradient in intensity can cause a bending movement towards the light due to dissimilar photo-induced stresses across the film thickness.[3,24–27] Although the deformation behaviour of photoresponsive LC-based actuators has been widely explored in air, relevant information for their integration in real devices, such as the capacity to exert forces and perform mechanical work upon light stimulation, has been addressed only in few occasions and further research is required.[9,23,28,29] Besides their use in air, the study of the performance of these materials within fluids is of great relevance for biomedical applications as said above, however, analysis of the deformation achieved upon light-stimulus in other media than air is limited, with the results reported to date being mainly focused on bending deformations generated by relatively low strains underwater.[3,10,15,24–27,30,31] Thus, further research to demonstrate the capacity of these materials to accomplish other mechanical functions beyond bending, such as contraction or expansion, when submerged in biologically relevant media, is required. This is especially important considering that actuation of azobenzene containing LC-based elements may be severely affected by the presence of fluids as they dissipate sample heat in a more efficient manner than air, considerably limiting the photothermal contribution to the mechanical response.[10]

Herein, we report an analysis of the light-induced mechanical actuation of thiol-acrylate-based azobenzene containing liquid crystal elastomers (LCEs), prepared by direct ink writing (DIW), when submerged in a biological buffer. We have chosen DIW as a newly developed relevant fabrication technique of these types

of actuators that can make their future integration in devices industrially feasible. This printing technique has demonstrated the manufacturing of LCE-based structures with digitally controlled molecular orientation, defined by the LC direction.[26,32–34] Printing of LC macromers leads to mesogen alignment along the printing direction that can be fixed through photopolymerization, leading to the structured LCE.[9,32–35] This precise control of the alignment of the printed materials allows programming the response, conferring the structures the ability to change their shape in a controlled manner in response to an external stimulus and leading to the so-called four-dimensional (4D) printing concept which adds time as the 4th dimension.[36–38] Although the fast mechanical response of this type of printed actuators has been reported upon photoirradiation in air, resulting in effective mechanical work, the mechanical performance of these direct ink-written actuators beyond bending characterization has not yet been studied in fluids.[9]

Regarding the fluid, we have chosen phosphate-buffered saline (PBS), a buffer solution, mainly containing water, sodium and potassium salts, that closely mimics ion concentrations, pH and osmolarity found in the human body. Being non-cytotoxic to most types of cells, PBS is a relevant fluid in many biological applications. The exploration of the photomechanical response of LCE-based actuators when submerged in this biological buffer is carried out in this paper. Additional experiments were performed in air and another model fluid to further understand the mechanisms underlying actuation in PBS.

2. Experimental section

Materials

1,4-Bis-[4-(3-acryloyloxypropyloxy)benzoyloxy]-2-methylbenzene (1, RM257) and 1,4-bis-[4-(6-acryloyloxyhexyloxy)benzoyloxy]-2-methylbenzene (2, RM82) were purchased from Merck. 4,4′-Bis(6-acryloyloxyhexyloxy) azobenzene (3, A6A) was purchased from Synthon. 3,6-Dioxa-1,8-octanedithiol (4, DODT) and 1,8-diazabicyclo [5.4.0] undec-7-ene (DBU) were obtained from Sigma-Aldrich. Photoinitiator Irgacure 819 (5) was purchased from Sigma-Aldrich. The dichloromethane (DCM) solvent was obtained from Biosolve. Polyvinyl alcohol (PVA) (80% hydrolyzed; M_w of 9000–10 000) was acquired from Aldrich. Fluorinert FC-40 was provided by Fluorochem (density: 1.855 g cm^{-3}) and PBS was obtained from Sigma-Aldrich.

Oligomer preparation

The oligomer was synthesized *via* a base-catalyzed thiol-acrylate Michael addition reaction. First, diacrylate mesogens RM82 and RM257, diacrylate azobenzene A6A and dithiol chain extender DODT were added in a flask and dissolved in DCM. Mole ratios were 2.275 : 2.275 : 0.45 : 4.5 for RM82 : RM257 : A6A : DODT. After mixing the components into a solution, two drops of DBU were added. The resulting mixture was stirred at room temperature overnight. After that, the DBU catalyst was removed by adding Amberlyst 15 ion exchange resin to the

4084 | *J. Mater. Chem. B*, 2023, **11**, 4083–4094

This journal is © The Royal Society of Chemistry 2023

reaction mixture. After 30 minutes of stirring, the reaction mixture was filtered and concentrated by rotary evaporation. Remaining solvent traces were removed *in vacuo* overnight. Finally, the oligomer (98 wt%) was mixed with the photoinitiator, Irgacure 819, at a proportion of 2 wt% in DCM. The final ink was obtained after removing the solvent at RT under a vacuum overnight.

3D Printing equipment

Light responsive samples were printed using a home-built 3D printer formed by a computer numerical controlled (CNC) router chassis with a built-in ink reservoir.[9,32] The reservoir, whose temperature is controlled and adjusted, is coupled to a dispensing needle tip. When pressure is applied on demand, the ink is extruded through the needle while describing X, Y and Z motions. Libre-Cad freeware software was used to generate computer-aided design (CAD) files. Printing was controlled by WinPC-NC software.

3D Printing of LCE structures

The ink, previously loaded in a reservoir connected to a needle tip (inner diameter of 0.33 mm), was heated to 80 °C and extruded on top of a PVA-coated glass microscope slide kept at RT. The PVA coating was prepared by dripping a solution of 5 wt% PVA and Milli-Q purified water on the glass substrates which were then left to dry at 60 °C for 60 min. The movement of the needle tip determines with precision the position of the deposited ink, drawing the geometry previously defined by CAD software. Contiguous parallel lines were printed at a speed of 0.8 mm s^{-1}, creating a dog bone shape with the oligomers aligned parallel to the long axis of the samples. Photoinduced polymerization of each sample was carried out by exposure to light from a 300 W Mercury lamp from Oriel (Model #6286); Lamp Housing also from Oriel (Model #66902), in conjunction with a UV reflecting filter (350–450 nm, Model #66218). The sample was positioned 20 cm from the lamp exit, using an additional long-pass optical filter with a cut-on wavelength of 390 nm, in order to minimize azobenzene stimulation, leading to a light intensity of 75 mW cm^{-2} on the sample. Each side of the sample was sequentially irradiated for 30 min until completion of a total curing time of 2.5 hours. During irradiation, the sample was maintained at 45 °C in a vacuum oven under a mild vacuum of 100 mbar.

Oligomer characterization

Proton nuclear magnetic resonance (^{1}H NMR) spectra were collected on a 400 MHz Bruker Advance III HD spectrometer with chloroform-d (purchased from Sigma-Aldrich Inc., 99.8 atom% D, 0.03% v/v tetramethylsilane). DSC measurements were employed to determine the transition temperature of oligomers in a TA Instruments DSC Q1000 system.

Molecular alignment characterization

The alignment of LC-printed samples was examined using a polarized optical microscope (POM) (Nikon Eclipse 80i).

Thickness characterization

The thickness of the printed elements was measured using the profilometer Bruker DektakXT Stylus Profiler.

Gel fraction

Samples for the gel fraction test were first printed and photopolymerized in PVA-coated glass slides of known mass. Next, samples were weighted and soaked in THF for 48 hours. Subsequently, the samples were removed from the solvent and left to dry for 4 hours in a vacuum oven at 70 °C. Afterwards, the weight of the sample was measured again. Gel fraction (GF) was calculated by

$$\text{GF}(\%) = \frac{W_\text{f}}{W_\text{i}} \times 100 \tag{1}$$

where W_f is the final weight of the sample after the unreacted material was dissolved and the remaining solvent was evaporated, and W_i is the initial weight of the sample, after the curing step and before being introduced in the solvent.

Thermo- and photoactuation characterization

Dog-bone-shaped samples, manufactured by extrusion printing of the described oligomeric ink, were used for subsequent thermo- and photoactuation experiments both in fluid and air. After extrusion and photopolymerization of the samples, they were immersed in water to dissolve the sacrificial PVA layer of the substrate and release the LCE actuators in a few hours. During the collection of the samples, both of their endings were attached to fixation tape for easier manipulation, leaving a rectangular testing area of 15 × 2.5 mm free for actuation. Then, samples were left to dry at RT.

Experiments using fluid media were performed in a metallic chamber with two opposing glass slides facing each other to facilitate light excitation and visual observation. A thermocouple, protected from the light beams, was immersed in the fluid for temperature monitoring of the media. Each sample, coupled to a metal weight of 1 g attached to one extreme, was placed inside the chamber after being filled with the corresponding media. When different media temperatures other than RT were required, the chamber was heated using a hot plate. Before starting the stimulation of the sample, the fluid temperature was thus increased and left to stabilize for 30 minutes. Experiments in air were performed in a homebuilt aluminium chamber. The chamber has two opposing cyclic olefin polymer (COP) windows as optical accesses to ensure good visibility of the actuation. A small hole of 5 mm of diameter was perforated in one COP film to allow local thermal monitoring of the surface of the sample using a thermographic camera (Gobi, from Xenics).

During thermoactuation experiments, the sample was heated up to 90 °C at a rate of 1 °C min^{-1} and subsequently left for cooling to 30 °C to check the reversibility of the actuation. For photoactuation experiments, depending on the specific requirements of each test, one or both sides of the sample were irradiated with UV LEDs (365 nm, 2 minutes of irradiation) first for excitation. Then, the samples were left in the dark for

This journal is © The Royal Society of Chemistry 2023

J. Mater. Chem. B, 2023, **11**, 4083–4094 | **4085**

2 minutes and, subsequently, one or two blue light LEDs (455 nm, 30 minutes of irradiation), depending on the illumination scheme, were used for relaxation. Additionally, light intensity passing through the transparent interfaces of the chambers was measured for air and fluid media before carrying out photoactuation experiments. From these measurements, a 5% additional decrease of the light intensity on the sample's surface was estimated to be introduced by the interfaces involved in the light-triggered experiments in air when compared to the experiments carried out in fluid. We have taken this attenuation into account to compensate for the intensity difference.

Actuation of the samples in fluid and air media was monitored by taking images every 5 °C or extracting images from the video recording acquired using a digital camera Nikon D3300 in thermoactuation and photoactuation experiments, respectively. The length of the actuator (L) was measured from the images by drawing and measuring a straight line along the long axis of the testing area of the sample, between both fixation tape endings. ImageJ free software was employed for the measurements. L_0 is defined as the initial length of the active area of the samples (between both fixation tapes at the endings) when coupled to the 1 g weight, for each experiment. In thermoactuation, length values at each temperature (L) were normalized by the initial length (L_0) while at 30 °C. On the other hand, length values (L) were normalized by the initial length (L_0) before UV light irradiation at RT or 37 °C, depending on the specific conditions of each one of the light-triggered experiments. Fractional contraction (C) is defined as $(L_0 - L)/L_0$.[17] For photoactuation experiments, fractional contraction (C) has been normalized to the maximum fractional contraction (C_{max}) achieved during UV light irradiation.

3. Results and discussion

Design and printing of LCE elements

An azobenzene containing a nematic LC oligomer with thiol-acrylate chemistry was employed to prepare LCE-based elements by DIW.[25] These elements will be later used in thermo- and photoactuation experiments. The oligomer precursor for printing was synthesized by a two-stage reaction consisting of a base-catalyzed thiol-acrylate Michael addition reaction followed by a photopolymerization step after DIW (Fig. 1a). In the first stage, the addition reaction, a mixture of mesogenic diacrylates, RM257 (1), RM82 (2) and A6A (3) were mixed with a non-mesogenic dithiol chain extender DODT (4) in a 10 : 9 molar ratio (acrylate:thiol). All these molecules are shown in the top part of Fig. 1a. The diacrylate mixture contains 9 mol% of azobenzene chromophore (A6A), the rest being RM82 and RM257, in a 1 : 1 molar ratio. An akin ink formulation, synthesized with RM82 diacrylates, was presented in the recent literature.[26] Thin fibres made from that ink showed anisotropic expansion at the illuminated side when irradiated with UV light, caused by a transition from smectic-C to smectic-A. However, in this work, by the introduction of irregularities in the spacer length using the combination of RM82 and RM257 mesogens in the oligomer, smectic phases are avoided
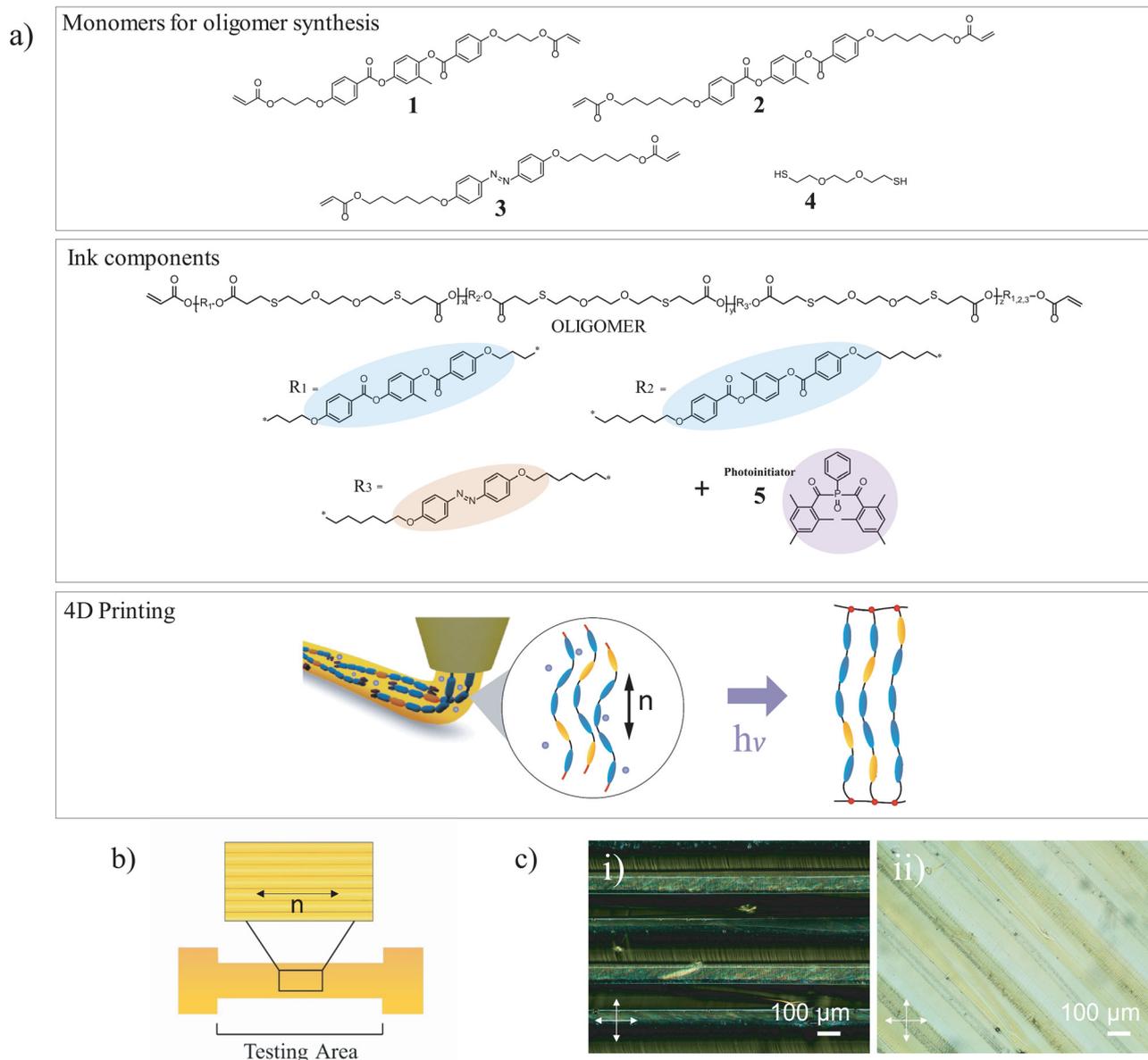
(see Differential Scanning Calorimetry, DSC, in Fig. S1, ESI†) and only linear strains are expected upon light stimulation.[39] The chromophore, A6A azobenzene was added during this first stage of the oligomer reaction to incorporate its molecules into the main chain, thus this configuration previously associated with an increased actuation.[25] A controlled excess of diacrylates in comparison with the dithiol extender was added to favour the formation of polymer chains with reactive acrylate groups at the ends (middle box of Fig. 1a), which promote the polymerization of the oligomer into a LCE by photoinitiated free-radical polymerization in the second stage. In order to trigger this last reaction, Irgacure 819 photoinitiator (5), shown in the middle box of Fig. 1a, was added to the ink at a proportion of 2 wt%.[25] Once the ink was prepared, physical and thermal properties of the material were characterized. The oligomer precursor had a number average molecular weight (M_n) of 7850 g mol^{-1} (obtained from Nuclear Magnetic Resonance, NMR, experiments) and DSC analysis revealed a T_g at −18.3 °C with a nematic to isotropic transition temperature (T_{NI}) at 78 ± 1 °C (see Fig. S1, ESI†).

LCE-based actuators with a dog-bone geometry were generated by DIW describing adjacent lines of ink parallel to the long direction of the stripe (Fig. 1b). Continuous samples, homogeneous in thickness, were achieved after the optimization of some relevant printing conditions such as needle diameter (0.33 mm), speed (0.8 mm s^{-1}), print head pressure (7 bars), as well as print head and substrate temperature (80 and 25 °C, respectively). Polarization optical microscopy (POM) images of these samples, observed with the printing direction at 0° and 45° with respect to the transmission direction of the first polarizer, showed a birefringent texture of the deposited material right after printing (Fig. 1c). These observations, with light extinction at 0° and light transmission at 45°, are compatible with a mesogenic orientation parallel to the printing direction, the long direction of the actuator, as previously described in the literature.[9,26,32–34] This orientation could be induced during the extrusion process through the shear forces applied in the needle and/or the elongational flow during the deposition of the material.[32] Then, the printed samples were photopolymerized following the curing protocol described in the experimental section to fix the induced molecular alignment, maintaining the same preferential uniaxial orientation direction after curing. Gel fraction tests were performed on samples printed and cured leading to values of 75 ± 5%.

Thermomechanical response of LCE actuators

Prior to performing photoactuation experiments, deformation under thermal stimulation was quantified to gain insight into the mechanical response of our samples when fully submerged in a PBS solution. This fluid is a water-based salt solution (pH ∼ 7.4) containing sodium and potassium salts. Density and thermal properties (specific heat capacity: 4000 J kg^{-1} °C at 25 °C; thermal conductivity: 0.58 W m^{-1} °C at 25 °C) are very similar to those of water.[40,41] The samples are fully immersed in the fluid to ensure a good thermal contact with the fluid also avoiding effects of the air–liquid interface.[42] In order to have data comparable to those of the photomechanical experiments

4086 | J. Mater. Chem. B, 2023, **11**, 4083–4094

This journal is © The Royal Society of Chemistry 2023

Fig. 1 (a) (top box) Molecular structure of the components to prepare the oligomer: diacrylate mesogens RM257 (1) and RM82 (2), diacrylate azobenzene A6A (3) and dithiol chain extender DODT (4). Blue elongated ovals represent the rigid core of the reactive mesogens, while orange ones represent that of the pro-mesogenic azobenzene. The purple circle represents the non-mesogenic photoinitiator. (Middle box) Ink components including the oligomer and the Irgacure 819 photoinitiator (5). The oligomer was synthesized via a base-catalyzed thiol-acrylate Michael addition reaction of the reactive mesogens and DODT. Mole ratios were 2.275 : 2.275 : 0.45 : 4.5 for RM82 : RM257 : A6A : DODT; photoinitiator (5) was added to the ink at a proportion of 2 wt%. (Bottom box) Ink printing and photocrosslinking of oligomers turning into a LCE. (b) Cartoon illustration of the geometry and printing direction of the samples, along the yellow lines, defining the director n (two-headed arrow). (c) POM images of the printed sample consistent in closely printed lines leading to a continuous strip. POM images were acquired between crossed polarizers (crosses indicate polarizer transmission directions) with the printing direction oriented (i) at 0° and (ii) at 45° with respect to the first polarizer transmission direction (scale bar = 100 μm).

(see the next section), the uniaxially oriented LCE elements were fixed at one extreme and a weight of 1 g was attached to their lower ending. In photomechanical experiments, this weight is applied to prevent the bending deformation upon UV light irradiation and precisely quantify the dimensions and shape changes of the LCE actuators. Besides, this experimental method provides data about the lifting capacity of the samples. It is important to note that it has been checked that for the studied actuators, these 1 g loads do not compromise the performance of the actuator, finding comparable thermo-mechanical contraction with unloaded samples within the experimental error while in air (Fig. S2, ESI†). The samples were heated from 30 °C to 90 °C while immersed in the buffer. The length of the samples (L) was measured every 5 °C, following the protocol described in the Experimental Section, and normalized by the initial length (L_0) at 30 °C. As a result of the thermal

This journal is © The Royal Society of Chemistry 2023
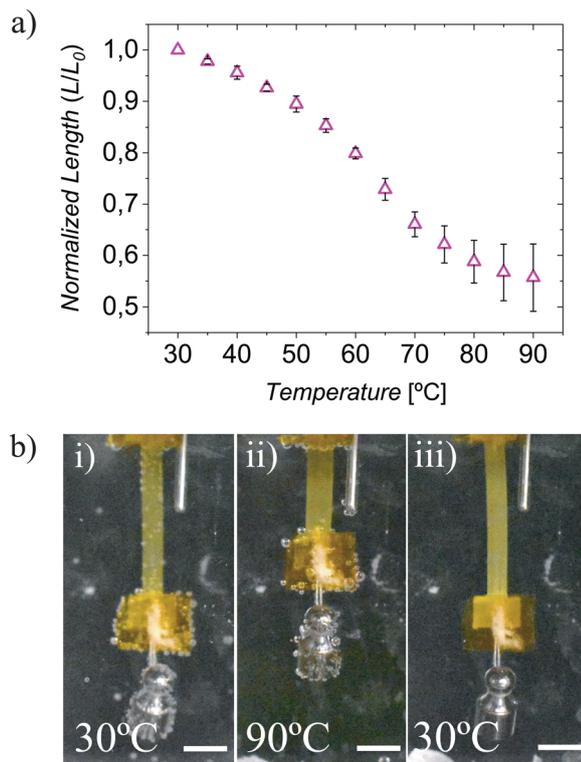
J. Mater. Chem. B, 2023, 11, 4083–4094 | 4087

a)

b)

Fig. 2 Thermomechanical response in PBS buffer of uniaxial oriented LCEs (65 ± 5 μm thick) with the director along its long axis. A load of 1 g attached to the extreme of the samples is lifted upon actuation. (a) Normalized length (L/L_0) of the LC elastomers during the heating from 30 °C to 90 °C. Mean ± SD of two samples. (b) Camera images collected at (i) 30 °C to (ii) 90 °C and after cooling down (iii) at 30 °C. Scale bar represents 5 mm.

stimulation, samples with an uniaxially oriented director (n), along the longitudinal axis of the sample, contract along this direction in the heating process which can be ascribed to a decrease of the mesogenic order, as previously described in the literature for uniaxial LCE samples (Fig. 2).[32,35] Between 50 and 80 °C, samples show a larger increase of deformation per degree of temperature reaching a mean value of 44% of contraction at 90 °C (Fig. 2a). This increase of the rate of contraction is tentatively associated with a greater disruption of the molecular order of the LCEs at this range of temperature. Afterwards, the samples were cooled to 30 °C obtaining a good recovery of the initial length values (typical recovery within ±1% of error) which demonstrated the reversibility of the actuation (Fig. S3, ESI†) in our 4D-printed elements. Furthermore, when comparing this result with experiments performed with a sample immersed in purified water (milliQ), similar contraction behaviour and magnitude were obtained, suggesting that the presence of salts in PBS media does not affect the overall thermomechanical response of the actuator upon thermal stimulation (Fig. S4, ESI†). Due to the higher density of PBS (1.01 g cm^{-3}) when compared to that of air (0.0013 g cm^{-3}), the metal weight coupled to the sample had a lower apparent weight of 0.89 g. With an active part mass of 4 mg, the prepared element can lift an object more than 200 times its own weight to a significant height (44% of the 15 mm initial length), just by heating the LCE sample to 90 °C. This highlights the capacity of these 4D-printed actuators to perform mechanical work.

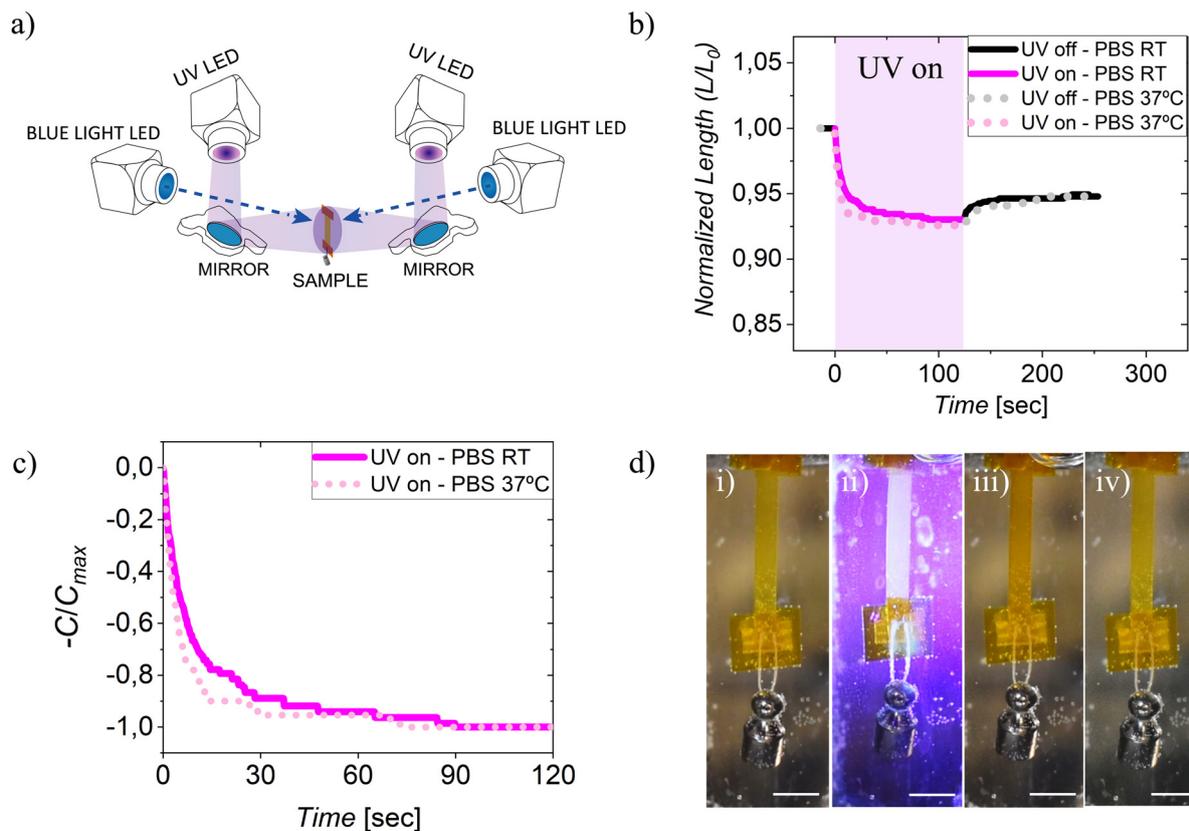### Photomechanical response of LCE actuators

Within the main purpose of this work, the mechanical response of our direct ink-written actuators under light stimulation was analysed when submerged in PBS, thus reporting new and potentially valuable data concerning the contractile behaviour of LCEs in physiological buffers. The sample is coupled, as mentioned above, to a metal weight of 1 g to inhibit the bending of the sample during irradiation and obtain net contractions. To avoid the impact of an asymmetric excitation on the photomechanical response, both sides of the sample were irradiated simultaneously by two UV LEDs (365 nm, 90 mW cm^{-2} on each sample surface) for excitation of the *trans* azobenzene isomers, and two blue light LEDs (455 nm, 3 mW cm^{-2} on each sample surface,) for photoinduced relaxation back of the *cis* to the *trans* isomers (Fig. 3a). Fig. 3b shows the normalized length when irradiating both sides of a sample for experiments carried out in the PBS solution at room temperature (RT). A maximum contraction of 7% of the initial length has been obtained after two minutes of UV light illumination. In addition, a decrease in the contraction was followed over a few seconds after the UV light was switched off, leading to a remnant contraction of 5% of the initial length, after leaving the sample in darkness for two minutes. This remnant deformation may be correlated with the presence of *cis* isomers with a long lifetime at RT. These results, with a small relaxation after UV light is switched off, and before the blue light is switched on, suggest a small UV photoinduced heating while in PBS, as this will be discussed later more in detail, and thus a predominance of the photochemical effect caused by the UV photoinduced isomerization of the azobenzene, as previously reported in other azo-containing soft actuators when actuating in fluids.[10,25]

For the employed azobenzene unit, substituted at the 4′-position with oxygen atoms, the *cis* isomer has a lifetime of several hours at RT.[43] However, isomerization back from the *cis* to the *trans* state for this chromophore can also be induced by irradiation with blue light.[21] Therefore, subsequent irradiation with blue light was carried out for 30 minutes, leading to the recovery of the initial length (within 1% of error), as *cis* isomers are isomerized back to the thermodynamically stable *trans* form as in the original film (Fig. S5, ESI†).

It is important to note that irradiation with UV light also led to a change in the colour of the sample.[9] While the thermodynamically stable azobenzene *trans* form leads to yellow-orange coloured films, the UV photogenerated *cis* isomers turn the film into dark orange. The irradiation of the sample with blue light leads to a recovery of the initial yellow-orange colour due to the isomerization of the *cis* back into the *trans* form.

If we focus back on the UV irradiation stage, considering the principle of energy conservation, the power leaving the sample during this UV irradiation stage, in the stationary state, must be the same as the luminous power that is being absorbed in the element.

4088 | *J. Mater. Chem. B*, 2023, **11**, 4083–4094

This journal is © The Royal Society of Chemistry 2023

Fig. 3 Photomechanical response in PBS of a uniaxial oriented sample (70 μm thick) with the director along its long axis. A metal weight of 1 g is attached to the lower extreme of the sample. (a) Experimental setup for photomechanical experiments. Irradiation is applied by two UV/blue LEDs irradiating both sides of the sample at equal intensities (90 mW cm^{-2} and 3 mW cm^{-2}, on each of the sample surfaces, for UV and blue light, respectively). (b) Normalized length (L/L_0) of the LCE during UV irradiation in PBS at RT (purple solid line) and at 37 °C (pink dotted line). The partial recovery of the length when UV illumination ceases is also shown for the experiments carried out at RT (black solid line) and at 37 °C (grey dotted line). (c) Normalized contraction expressed in negative values ($-C/C_{max}$) during exposure to UV light in PBS at RT (solid line) and 37 °C (dotted line). Normalized contraction is given in negative values to show the dynamic as a decay. (d) Images of the LCE element successively acquired (i) before UV illumination, (ii) after UV illumination (after 2 min of illumination with 90 mW cm^{-2} of UV light on each of the sample surfaces), (iii) 2 min after ceasing the UV illumination, (iv) after blue light irradiation (3 mW cm^{-2} on each of the sample surfaces) while in PBS at 37 °C. Scale bar represents 5 mm.

Although gradients in the sample are anticipated due to the non-homogenous intensity profile in the sample and the contact with fluid, it might be expected that the average temperature reached at this stationary stage of the irradiation could have a direct relationship with the intensity reaching the sample and an inverse one with the thermal conductivity of the surrounding medium that relates to the rate of evacuation of heat from the sample.[44] Thus, the increment of the sample's temperature during irradiation in a medium like PBS with a high thermal conductivity, compared to that of air, is such that the removal of the light stimulus leads to a small loss of contraction of only 2% of the initial length of the sample. Taking into consideration the contraction of our samples during thermoactuation experiments in PBS (Fig. 2), and assuming that this loss of contraction upon UV removal could be mainly related to the elimination of the photothermal contribution, we can estimate that such an extra contraction of 2% upon UV illumination may represent a temperature increment of around 5 °C. It has to be noted that, when making this estimation, microstructure differences between the photoirradiated and the unexposed LCE are not

considered. That is, UV light stimulation of the polymer leads to the presence of a *cis* population. Besides, while irradiated, the polymer is also subjected to continuous *trans-cis-trans* isomerization cycling as well as to additional and relevant gradients within the sample, as it is being photoheated within a fluid with good heat withdrawing capacity. In contrast, when the sample is actuated by a thermal stimulus, the azobenzene chromophore is in the all-*trans* state and the fluid temperature is homogeneous and equal to that of the sample. Nevertheless, despite all these assumptions, the small changes in contraction upon UV removal make plausible the estimation of a small photoinduced temperature increase of the sample of only a few degrees Celsius during the UV irradiation stage within the PBS fluid. Regarding the dynamics of the photoactuation under UV irradiation in PBS, it is remarkable that 50% of the maximum contraction value was quickly reached in just 5 seconds (Fig. 3c).

Furthermore, within the scope of our article, covering the potential of these actuators in biomedical applications, the photoinduced actuation of the LCE elements was also studied when the PBS fluid was at a human body temperature of 37 °C.

This journal is © The Royal Society of Chemistry 2023

J. Mater. Chem. B, 2023, **11**, 4083–4094 | **4089**

Due to this increment of temperature, a contraction of around 3% with respect to the initial length at 30 °C can be estimated according to the thermomechanical experiments shown previously, leading to an initial length, for this experiment, of roughly 97% of the initial length displayed at 30 °C. In Fig. 3b, the photomechanical response represented by the normalized length of the LCE element when in PBS at 37 °C can be observed, along with its comparison with the same media and irradiation scheme while at RT. The result reveals similar qualitative behaviour for the experiment carried out at 37 °C and similar values of the maximum contraction, when compared to that performed at RT, demonstrating a mechanical work capacity of about 2 J kg^{-1} in these experiments. After switching off the UV LEDs, the contraction decreases and a remnant contraction of 5% in the sample was achieved (Fig. 3b), which was forced back to the initial dimensions by irradiation with blue light (Fig. 3d and Fig. S5, ESI†). Regarding dynamics, faster contraction speed to that measured in photo-actuation experiments carried out in this same medium at RT was detected at 37 °C, achieving 50% of the maximum contraction after only 3 seconds (Fig. 3c). The faster response at 37 °C could be explained by a higher molecular mobility at this higher temperature. As for some applications, a simpler irradiation setup may be desirable, and these experiments were replicated upon photostimulation of one side of one LCE element (Fig. S6a, ESI†) with a 1 g metal weight to identify, if present, dissimilar photoinduced stresses across the film thickness that could lead to differences in the mechanical performance (magnitude of the contraction and its dynamics) in comparison to results with the two LEDs configuration. In order to reproduce the same total photon dosage throughout the experiments with both irradiation configurations, UV and blue LEDs irradiating only one face of the sample were adjusted to double the intensity used with each LED during the main experiment with two UV/blue LEDs irradiating both faces. Figs. S7 and S8 (ESI†) show the normalized length as well as the normalized contraction when actuation takes place in PBS buffer at RT and 37 °C, respectively, under irradiation of only one side of the sample. During UV irradiation of one face of the

sample at 180 mW cm^{-2}, maximum contractions while in PBS, at RT and at 37 °C, were 7% and 8%, respectively. 50% of these contraction values were achieved after about 5 and 3 seconds of switching on of UV light (single LED), for RT and 37 °C, respectively, thus resulting in similar response times to those found for the experiments with two LEDs.

When comparing the results of both irradiation configurations (illumination of one or both sides of the sample), a similar pattern of contraction speed towards the stationary value and contraction magnitudes was obtained, which is likely due to a similar total dose of UV light received by the samples. Although it might not be discarded that the differences in the light spatial distribution in the sample, for one side *vs.* two sides experiments, could introduce different temperatures and indeed also different *cis* population spatial distributions within the sample, these seem to have a marginal impact on the photomechanical response of the illuminated element while in the PBS fluid, given the very similar dynamics found for both configurations.

It is worth noting that these cycles of excitation/relaxation of one/both faces of the sample at room temperature and body temperature were successively repeated, up to five times, obtaining similar deformations and thus validating the integrity of the material under repeated cycle actuation.

The studies presented so far have demonstrated that the actuation in PBS, at our light intensity regimes, is mainly governed by the photochemical contribution caused by the isomerization of the azobenzene, as the photoinduced heating of the samples is diminished by the fluid, which acts as a heat sink and takes heat from the sample efficiently.[10,27]

To better understand the relationship between the photomechanical behaviour and the surrounding media in which the sample is immersed, experiments similar to those previously shown in PBS, but in other media of significantly different thermal properties, were carried out. Photoactuation in air was first analysed as this has a significantly different thermal conductivity, 23 times smaller than that of PBS. Thermoactuation experiments while in air revealed comparable results than those obtained in PBS and to values previously shown in the
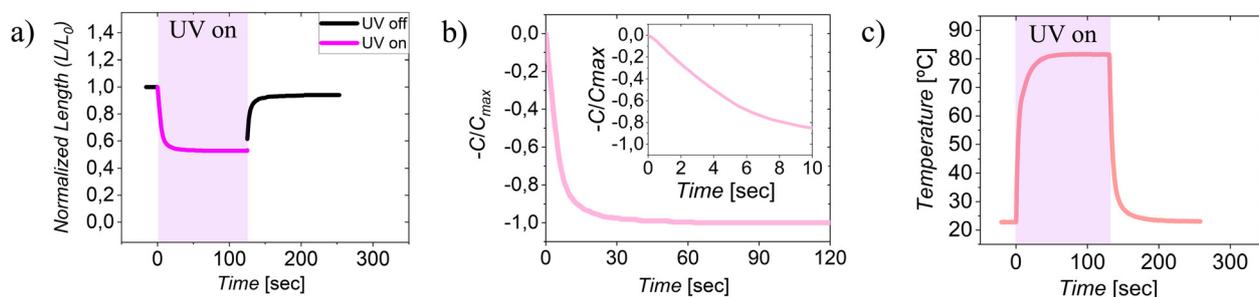

Fig. 4 Photomechanical response in air at RT of a uniaxial oriented sample (70 μm thick) with the director along its long axis. A metal weight of 1 g is attached to the lower extreme of the sample. (a) Normalized length (L/L_0) of the LC elastomer during UV irradiation (purple line) in air using two UV LEDs irradiating each face of the sample with an intensity of 90 mW cm^{-2} and subsequent partial recovery of the length when UV illumination ceases (black line). (b) Normalized contraction expressed in negative values ($-C/C_{max}$) during exposure to UV light. Normalized contraction is given in negative values to show the dynamic as a decay. (b inset) Detail of the normalized contraction, in negative values, during the first 10 seconds of UV light irradiation. (c) Temporal dependence of the temperature of the LCE surface during UV light irradiation (purple square) and after switching off the UV illumination.

4090 | *J. Mater. Chem. B*, 2023, **11**, 4083–4094

This journal is © The Royal Society of Chemistry 2023

literature (Fig. S9, ESI†).[9,32,34] Fig. 4a shows the normalized length when irradiating both sides of a sample for experiments carried out in air. A maximum contraction of 47% of the initial length when irradiating two sides of the sample was achieved, requiring 4 seconds to reach 50% of that value (Fig. 4b).

The temperature of the samples was measured using a thermographic camera. The fast and large deformation during the first few seconds of UV light irradiation is accompanied by a fast and large temperature increment up to 81 °C (Fig. 4c). After switching off the light, the deformation rapidly decreases and a remnant contraction of 6% of the initial sample length is observed while the temperature quickly relaxes to RT in the absence of any light excitation. Subsequently, after the period in the dark, irradiation with blue light was started leading to the recovery of the initial length (within 1% of error) (Fig. S5, ESI†). Comparable maximum temperature values (79 °C) and maximum and remnant contractions (45% and 6%, respectively) were measured when irradiating only one side of the sample at a similar total photon dosage compared to experiments carried out with two LEDs (Fig. S10, ESI†). These comparable temperature values might indicate that the rate of transfer of energy to the surrounding air is similar in both configurations in the stationary state, leading to similar mechanical responses too.

The observed photoinduced behaviour in air can be explained by the photothermal and photochemical contributions to the contraction of the sample, previously described in the literature.[9,10,15,16,20–22,27] The important photoinduced temperature increment of the sample during UV irradiation contributes to its contraction due to a heat-induced disorder of the mesogens, being especially important in magnitude for the high-intensity regime used in our experiments. On the other hand, the photoinduced generation of *cis* isomers also contributes to this disorder. When UV light is switched off, the temperature relaxes in a few seconds, so the thermal contribution to the contraction also decreases while the presence of azobenzene molecules in their *cis* state explains the remnant contraction.[9,26,27] The magnitude of this remnant contraction is similar for both light exposure configurations (irradiation of one or both sides of the sample) which could be tentatively ascribed to a similar population of *cis* isomers reached after UV illumination and temperature relaxation processes although a different spatial distribution is expected. Interestingly, during thermoactuation (Fig. S9, ESI†), samples contracted around 36% at 80 °C when carrying the same load, which is below the contraction reached by exposure to UV light (45–47%), for both one or two LEDs configurations. Such a difference could be tentatively related to the photochemical contribution to the actuation, not present in thermoactuation experiments.

Subsequently, photomechanical behaviour was studied in a third media, a fluorinated fluid (Fluorinert FC-40) that has thermal properties between those of air and PBS (specific heat capacity: 1100 J kg⁻¹ °C at 25 °C; and thermal conductivity: 0.065 W m⁻¹ °C at 25 °C) to further research the effect of these properties on the mechanical actuation of our actuators in liquid media. As a prior reference, deformation behaviour under thermoactuation was checked, showing a trend similar
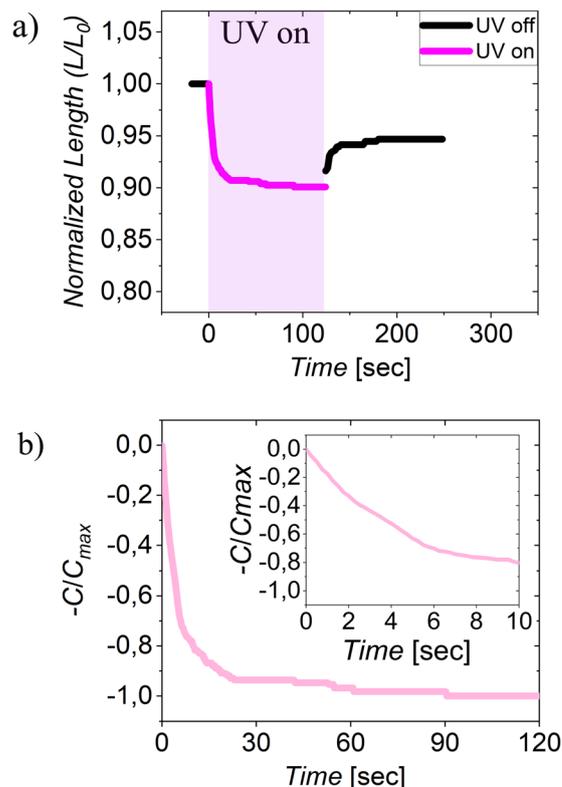

Fig. 5 Photomechanical response in FC-40 at RT of a uniaxial oriented sample (70 μm thick) with the director along its long axis. A metal weight of 1 g is attached to the lower extreme of the sample. (a) Normalized length (L/L_0) of a uniaxial oriented sample (70 μm thick) with the director along its long axis during UV irradiation (purple line) using two UV LEDs (90 mW cm⁻² on each of the sample surfaces) for the irradiation of both sides of the sample and the partial recovery of the length when UV illumination ceases (black line). (b) Normalized contraction expressed in negative values ($-C/C_{max}$) during exposure to UV light. Contraction is given in negative values to show the dynamic as a decay. (b inset) Detail of the normalized contraction, in negative values, during the first 10 seconds of UV light irradiation.

to PBS and air (Fig. S9, ESI†). Regarding photoactuation, using two LEDs for irradiation of both sides of the sample, a contraction of 10% with respect to the initial length (Fig. 5a), much lower than the contraction obtained in air but larger than that reached in PBS, was achieved under the same irradiation conditions. While the relaxation of the contraction was around 2% of the initial length when UV light is switched off in the experiments carried out in PBS at RT, a change of 5% of the contraction of the initial length of the sample can be observed when suppressing the UV irradiation in the fluorinated fluid. In analogy with the experiments carried out in air and in PBS, this relaxation could be ascribed to temperature relaxation, and the remnant deformation after switching off the UV light may be correlated with the presence of *cis* isomers with a long lifetime at RT. Fluorinert FC-40, with a thermal conductivity 9 times smaller than PBS, dissipates less efficiently the heat generated in the sample, enabling a higher temperature to be reached by the sample during the UV irradiation period, this could explain the higher stationary value of the contraction in this medium.

This journal is © The Royal Society of Chemistry 2023

J. Mater. Chem. B, 2023, **11**, 4083–4094 | **4091**

Considering contraction values shown during thermoactuation experiments in this fluid, the additional contraction of 5% of the initial length observed during UV irradiation with respect to the remnant contraction after the UV light stimulation period could represent an increment of the temperature of approximately 15 °C in the sample. A 50% of the UV photoinduced contraction was reached in just 4 s (Fig. 5b), which is faster than that in PBS under the same irradiation conditions at RT and similar to that in air. Minor differences between the dynamics of PBS and FC-40 at RT could be ascribed to the photothermal contribution to the contraction that is significant in the experiments carried out in Fluorinert FC-40 in addition to the photochemical effect, while in experiments in PBS, the photochemical contribution dominates.

The previously shown studies, carried out in air and in a fluorinated liquid, with thermal conductivities 23 and 9 times smaller than that of PBS, respectively, showed contractions of 47% and 10% during the UV exposure step, respectively, highlighting the relevance of the thermal properties of the medium in the photomechanical response.

For all the studied media, PBS, air and Fluorinert FC-40, the photochemical contribution is in the order of 5–6% contraction of the initial length. Though these values are lower than those previously reported in the literature for photochemically induced contractions carried out in air, the LCE 4D-printed actuators presented in this work represent promising digitally fabricated photoresponsive systems to operate in fluids and under physiological conditions.[17,45] Further optimization can be easily pursued by improving the order achieved during processing and optimizing the polymer chemistry and/or the azobenzene content.

4. Conclusions

In this work, the photomechanical actuation in a biological buffer of azobenzene containing LCE elements prepared by 4D printing has been explored. Significant photoinduced contractions of the samples under load, in the range of 7% of their initial length, and therefore, effective photomechanical work performed by the actuators, have been demonstrated in a PBS buffer at RT. These actuators, of only a few milligrams, were able to rise to these heights, loads many times heavier than their own weight (more than 200 times), without impairing the integrity of the LCEs over several cycles.

Actuation at human body temperature led to similar contraction values than those reached at RT; however, dynamics was significantly favoured faster by the molecular mobility at this higher temperature. Importantly, the photomechanical response of these actuators in PBS is similar to that observed in Milli-Q water, indicating that these actuators are highly insensitive to the presence of salts in the buffer, this being advantageous with respect to hydrogels, whose response is highly dependent on the composition of the fluid.

Although photochemical and photothermal contributions can be identified in the photomechanical response of our actuators in PBS, under the studied conditions, the photothermal contribution is smaller than the photochemical one, despite the range of intensities employed (180 mW cm^{-2}). PBS efficiently dissipates the photoinduced heat of the sample, transferring this energy to the medium, leading to lower photothermal contributions that relax when UV light excitation ceases. In contrast, the photochemical contribution to the contraction, around 5% of the initial length, caused by the isomerization of the azobenzene units contributes to the contraction that remains after the UV light is switched off. The sample can be returned to the original length by exposure to blue light that reverts azobenzene *cis* isomers to the *trans* state. Equivalent studies carried out in air and in a fluorinated liquid, having these significantly different thermal conductivities, further confirm the importance of the photomechanical response of the thermal properties of the medium that drains heat from the sample reducing the photothermal contribution to the contraction. Irrespective of the medium, the photochemical contribution is in the same range of values, in the order of 5–6% contraction of the initial length.

It has also been shown that in the direct ink-printed elements, and for the regime of light intensities and wavelengths of excitation employed, the asymmetry introduced by irradiating only one single side of the sample, which could lead to stresses between the two actuator sides, does not produce significant differences in the magnitude of the photodeformation in the stationary state or in its dynamics when it is compared with schemes using irradiation of the two sides of the element with similar total photon dosages. These observations are valid both for air and PBS and they are relevant for the future applications of these soft photoactuators.

Despite not specifically designed for this purpose and out of the scope of our work, the reversible response of these LCE-printed actuators under physiological conditions may facilitate these actuators' application in mimicking the contractile behaviour of certain tissues, such as gut, with biologically relevant contractions of 5–10% of the initial length and response times in the order of a few seconds, offering an alternative to overcome the limitations observed in hydrogels, in terms of mechanical strength and actuation rates.[46] It is noted that local temperatures achieved by the LCE upon UV light irradiation at high intensities while in PBS, as in our experiments, were estimated to be around 5 °C. Though this value might not be suitable when handling cells, and light irradiation schemes might need to be optimized to make them compatible with living systems, this study may be a starting point for a further improvement of this material toward this type of application. To sum up, the described reversible contractile movements of our 4D-printed actuators, with time responses of a few seconds, demonstrated in a physiological environment (PBS) and at physiological temperatures, allow us to envision the use of these 4D-printed elements in the areas of microfluidics, soft robotic or biomedical applications.

Author contributions

C.S.-S. and A.P.H.J.S. conceived the research. D.J.M. and A.P.H.J.S. conceived the materials. D.J.M. synthesized the

4092 | *J. Mater. Chem. B*, 2023, **11**, 4083–4094

This journal is © The Royal Society of Chemistry 2023

materials. L.C., D.J.M., Z.K., A.P.H.J.S. and C.S.-S. set up the methodology. L.C. and M.L.-V. performed the experiments and analysed the experimental results. All authors discussed the experimental results. L.C. and C.S.-S. composed the first draft. All authors reviewed and improved the initial draft and approved the final manuscript.

Conflicts of interest

There are no conflicts to declare.

Acknowledgements

Notes and references

1 J. ter Schiphorst, J. Saez, D. Diamond, F. Benito-Lopez and A. P. H. J. Schenning, *Lab Chip*, 2018, **18**, 699.

2 A. Sánchez-Ferrer, T. Fischl, M. Stubenrauch, A. Albrecht, H. Wurmus, M. Hoffmann and H. Finkelmann, *Adv. Mater.*, 2011, **23**, 4526.

3 C. L. van Oosten, C. W. M. Bastiaansen and D. J. Broer, *Nat. Mater.*, 2009, **8**, 677.

4 R. Xiao and W. M. Huang, *Macromol. Biosci.*, 2020, **20**, 2000108.

5 S. Palagi and P. Fischer, *Nat. Rev. Mater.*, 2018, **3**, 113.

6 M. Sitti, H. Ceylan, W. Hu, J. Giltinan, M. Turan, S. Yim and E. Diller, *Proc. IEEE*, 2015, **103**, 205.

7 S. Coleman, J. ter Schiphorst, A. Ben Azouz, S. Bakker, A. P. H. J. Schenning and D. Diamond, *Sens. Actuators, B*, 2017, **245**, 81.

8 Y. Qiu and K. Park, *Adv. Drug Delivery Rev.*, 2001, **53**, 321.

9 L. Ceamanos, Z. Kahveci, M. López-Valdeolivas, D. Liu, D. J. Broer and C. Sánchez-Somolinos, *ACS Appl. Mater. Interfaces*, 2020, **12**, 44195.

10 M. Pilz da Cunha, E. A. J. van Thoor, M. G. Debije, D. J. Broer and A. P. H. J. Schenning, *J. Mater. Chem. C*, 2019, **7**, 13502.

11 M. Warner, *Annu. Rev. Condens. Matter Phys.*, 2020, **11**, 125.

12 Y. Xiao, Z. Jiang and Y. Zhao, *Adv. Intell. Syst.*, 2020, **2**, 2000148.

13 T. J. White and D. J. Broer, *Nat. Mater.*, 2015, **14**, 1087.

14 Y. Yu, M. Nakano and T. Ikeda, *Nature*, 2003, **425**, 145.

15 S. Palagi, A. G. Mark, S. Reigh, K. Melde, T. Qiu, H. Zeng, C. Parmeggiani, D. Martella, A. Sanchez-Castillo, N. Kapernaum, F. Giesselmann, D. S. Wiersma, E. Lauga and P. Fischer, *Nat. Mater.*, 2016, **15**, 647.

16 M. Pilz da Cunha, M. G. Debije and A. P. H. J. Schenning, *Chem. Soc. Rev.*, 2020, **49**, 6568.

17 H. Finkelmann, E. Nishikawa, G. G. Pereira and M. Warner, *Phys. Rev. Lett.*, 2001, **87**, 015501.

18 Z. Mahimwalla, K. G. Yager, J. Mamiya, A. Shishido, A. Priimagi and C. J. Barrett, *Polym. Bull.*, 2012, **69**, 967.

19 Z. Cheng, S. Ma, Y. Zhang, S. Huang, Y. Chen and H. Yu, *Macromolecules*, 2017, **50**, 8317.

20 D. Liu, C. W. M. Bastiaansen, J. M. J. den Toonder and D. J. Broer, *Angew. Chem., Int. Ed.*, 2011, **51**, 892.

21 D. Liu and D. J. Broer, *Nat. Commun.*, 2015, **6**, 8334.

22 A. H. Gelebart, D. Jan Mulder, M. Varga, A. Konya, G. Vantomme, E. W. Meijer, R. L. B. Selinger and D. J. Broer, *Nature*, 2017, **546**, 632.

23 T. Guo, A. Svanidze, X. Zheng and P. Palffy-Muhoray, *Appl. Sci.*, 2022, **12**, 7723.

24 A. H. Gelebart, M. Mc Bride, A. P. H. J. Schenning, C. N. Bowman and D. J. Broer, *Adv. Funct. Mater.*, 2016, **26**, 5322.

25 L. Liu, M. del Pozo, F. Mohseninejad, M. G. Debije, D. J. Broer and A. P. H. J. Schenning, *Adv. Opt. Mater.*, 2020, **8**, 2000732.

26 M. del Pozo, L. Liu, M. Pilz da Cunha, D. J. Broer and A. P. H. J. Schenning, *Adv. Funct. Mater.*, 2020, **30**, 2005560.

27 M. Pilz da Cunha, H. S. Kandail, J. M. J. den Toonder and A. P. H. J. Schenning, *Proc. Natl. Acad. Sci. U. S. A.*, 2020, **117**, 17571.

28 C. Ferrantini, J. M. Pioner, D. Martella, R. Coppini, N. Piroddi, P. Paoli, M. Calamai, F. S. Pavone, D. S. Wiersma, C. Tesi, E. Cerbai, C. Poggesi, L. Sacconi and C. Parmeggiani, *Circ. Res.*, 2019, **124**, e44.

29 M. Yamada, M. Kondo, J. Mamiya, Y. Yu, M. Kinoshita, C. J. Barrett and T. Ikeda, *Angew. Chem., Int. Ed.*, 2008, **47**, 4986.

30 C. Huang, J. Lv, X. Tian, Y. Wang, Y. Yu and J. Liu, *Sci. Rep.*, 2015, **5**, 17414.

31 M. Camacho-Lopez, H. Finkelmann, P. Palffy-Muhoray and M. Shelley, *Nat. Mater.*, 2004, **3**, 307.

32 M. López-Valdeolivas, D. Liu, D. J. Broer and C. Sánchez-Somolinos, *Macromol. Rapid Commun.*, 2017, **39**, 1700710.

33 C. P. Ambulo, J. J. Burroughs, J. M. Boothby, H. Kim, M. R. Shankar and T. H. Ware, *ACS Appl. Mater. Interfaces*, 2017, **9**, 37332.

34 A. Kotikian, R. L. Truby, J. W. Boley, T. J. White and J. A. Lewis, *Adv. Mater.*, 2018, **30**, 1706164.

35 M. del Pozo, J. A. H. P. Sol, A. P. H. J. Schenning and M. G. Debije, *Adv. Mater.*, 2021, **34**, 2104390.

36 C. Sánchez-Somolinos, *Mechanically Responsive Materials for Soft Robotics*, ed. H. Koshima, Wiley-VCH, Weinheim, Germany, 2020, Ch. 14, pp. 347–360.

37 S. Tibbits, *Archit. Des.*, 2014, **84**, 116.

38 D. Sun, J. Zhang, H. Li, Z. Shi, Q. Meng, S. Liu, J. Chen and X. Liu, *Polymers*, 2021, **13**, 1889.

39 M. O. Saed, R. H. Volpe, N. A. Traugutt, R. Visvanathan, N. A. Clark and C. M. Yakacki, *Soft Matter*, 2017, **13**, 7537.

40 O. Pakhomov, T. Gurina, V. Mazaeva, A. Polyakova, B. Deng, E. Legach and G. Bozhok, *Cryobiology*, 2022, **107**, 13.

This journal is © The Royal Society of Chemistry 2023

J. Mater. Chem. B, 2023, **11**, 4083–4094 | **4093**

41 F. Gielen, F. Pereira, A. J. deMello and J. B. Edel, *Anal. Chem.*, 2010, **82**, 7509.

42 S. Ma, X. Li, S. Huang, J. Hu and H. Yu, *Angew. Chem., Int. Ed.*, 2019, **58**, 2655.

43 G. Kumar and D. Neckers, *Chem. Rev.*, 1989, **89** 1915.

44 D. Bäuerle, *Laser Processing and Chemistry*, Springer, Berlin, Heidelberg, 2013.

45 M.-H. Li, P. Keller, B. Li, X. Wang and M. Brunet, *Adv. Mater.*, 2003, **15**, 569.

46 H. Kim, D. Huh, G. Hamilton and D. E. Ingber, *Lab Chip*, 2012, **12**, 2165.

4094 | *J. Mater. Chem. B*, 2023, **11**, 4083–4094

This journal is © The Royal Society of Chemistry 2023